Leibniz-Institut für Sonnenphysik (KIS)

FACULTY OF MATHEMATICS AND PHYSICS Charles University

Astronomical Institute of the Czech Academy of Sciences

THE ROLE OF MAGNETIC FIELDS IN THE EVOLUTION OF PORES

Marta García Rivas[1,2], Jan Jurčák[1], Nazaret Bello González[3]

[1]Astronomical Institute of the Czech Academy of Sciences, [2]Astronomical Institute of Charles University, [3]Leibniz-Institut für Sonnenphysik (KIS)

ESPM-16

Motivation

Does Jurčák criterion apply to other magnetic structures?

Jurčák criterion: Empirical law that states that umbra-penumbra (UP) boundaries of stable sunspots can be defined by a vertical magnetic field threshold that matches the continuum intensity boundary. This criterion implies that in regions with $|B_{ver}| > B_{crit}$, umbral mode of convection prevails. On the other hand, regions with $|B_{ver}| < B_{crit}$ are unstable and prone to vanish against other modes of magneto-convection.

Formation of sunspots:
UP boundary migrates towards the center of the umbra until it reaches a stable position. $|B_{ver}|$ on the boundary increases during the migration until it stabilizes, i.e., penumbra invades only umbral areas with weak $|B_{ver}|$.

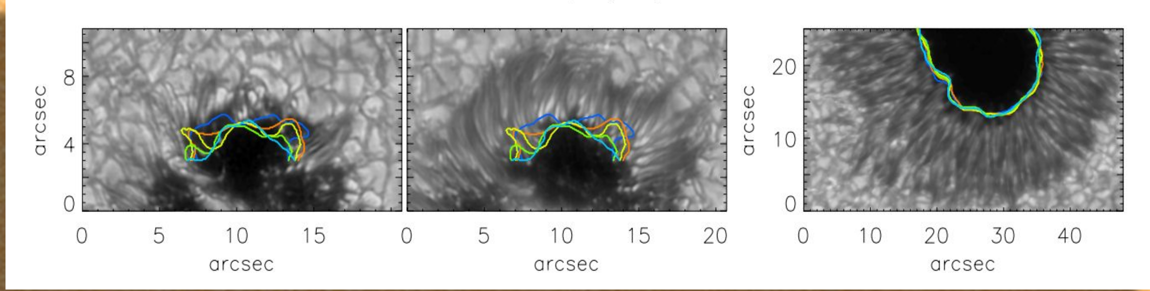

Figure 1: Dark blue to light blue, variation of the UP boundary with time in forming (left and middle) and stable sunspots. Jurčák et al. (2015)

Stable sunspots:
UP boundaries fluctuate around a mean position due to the dynamical properties of penumbral filaments. $|B_{ver}|$, however, remains constant.

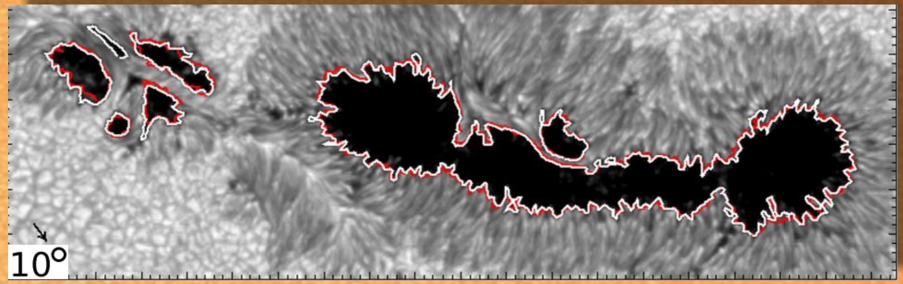

Figure 2: Stable sunspot with intensity and magnetic contours. $I_c = 0.5\ I_{QS}$ in white. $B_{ver} = 1867$ G in red. Jurčák et al. (2018)

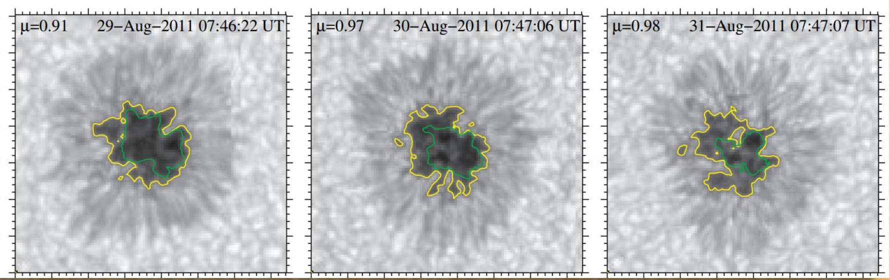

Decaying sunspots:
UP boundary migrates towards the center of the umbra until the sunspot disappears. $|B_{crit}|$ contour is located well inside the umbral area and it migrates towards the center of the umbra. The mean $|B_{ver}|$ gets weaker.
Figure 3: Decaying sunspot with intensity and magnetic contours. $I_c = 0.5\ I_{QS}$ in yellow. $B_{ver} = 1867$ G in green. Benko et al. (2018)

Data and methodology

Requirements:
- Infer vector magnetic field → Spectropolarimeter
- Study boundary conditions → Medium to high spatial resolution
- Study temporal evolutions → Temporal cadence smaller than lifetimes of pores
- A homogeneous database → Space-based

HMI@SDO

Pixel size: 0.5''

Temporal cadence: 12 min

Line: Fe I 617.3 nm

Selected data: The Helioseismic and Magnetic Imager (HMI), provides **full disc** Stokes parameters that are inverted using a Milne-Eddington code (VFISV, Borrero et al. 2011) to provide photospheric physical parameters. The standard spatial resolution of ~1'' can be improved by correcting the data for scattered light, i.e., data are deconvolved using a HMI PSF model. Therefore, we analyse **hmi.B_dconS** and **hmi.Ic_dconS** data series processed and provided by A. Norton.

The **boundary** of the structures are defined by a continuum intensity threshold (**0.55 I_{QS}**) and magnetic properties along the isocontour are averaged. **Magnetic thresholds** are defined based on the averaged boundary properties.

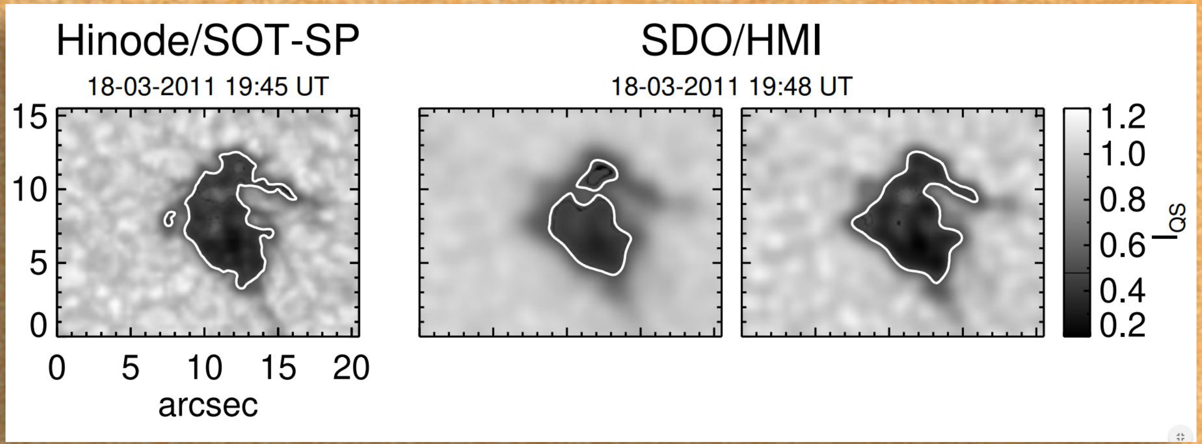

Figure 4: Motivation to use HMI deconvolved data. Continuum intensity images of the studied solar pore on 18 March. $I_C = 0.55\ I_{QS}$ contours in white. *Left*: Pore scanned at 19:48 UT with the spectropolarimeter onboard **Hinode**. *Middle*: **Standard HMI** map of the pore observed at 19:45 UT. *Right*: **Deconvolved HMI** map of the pore observed at 19:45 UT. García-Rivas et al. 2021

Case study: Lifetime of a pore

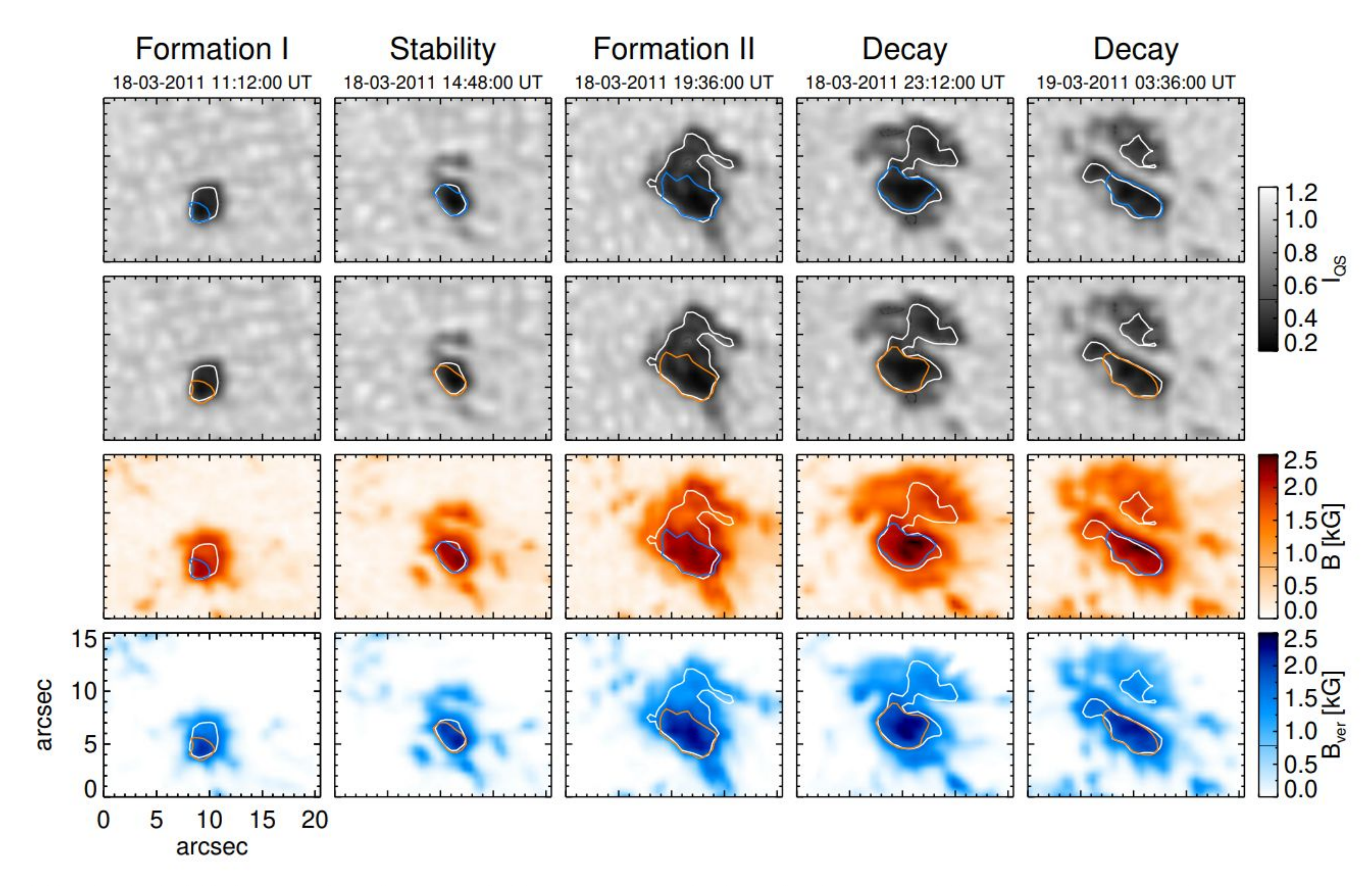

The studied solar **pore** appeared in the active region **NOAA 11175**. It is analysed during a **26.5-hour** span: from 09:24 UT on 18 March to 12:00 UT on 19 March 2011.

Figure 5: The pore at different evolutionary stages during its lifetime. Top two rows: Deconvolved continuum intensity maps. Third row: Magnetic field strength. Bottom row: Vertical magnetic field. White lines mark the analysed boundary (0.55 I_{QS}). Blue lines mark the total magnetic field threshold (B_{crit} = 1921 G) and orange lines mark the vertical magnetic field threshold ($B_{ver,crit}$ = 1731 G). The evolutionary stage of each frame is specified on top. García-Rivas et al. 2021

Results

In this case study, the pore exhibits a **stable phase (Sta)**. The maximum B_{ver} value, observed during the stable phase, is comparable to the maximum B_{ver} value found on UP boundaries. Therefore, we consider the mean B and B_{ver} during the stability stage as **magnetic critical thresholds** for the analysis (**B_{crit} = 1921 G; $B_{ver,crit}$ = 1731 G**).

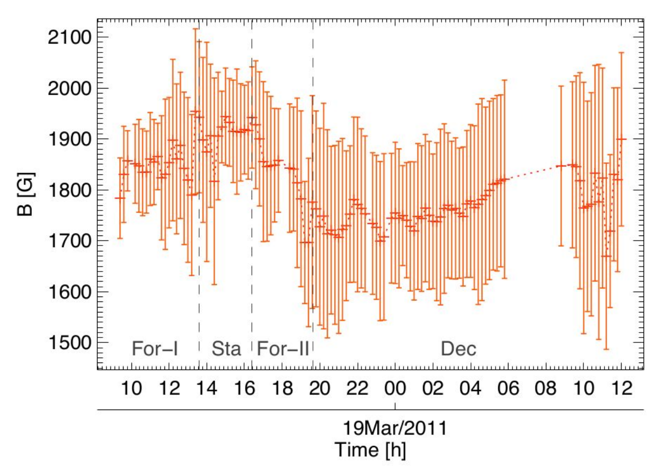

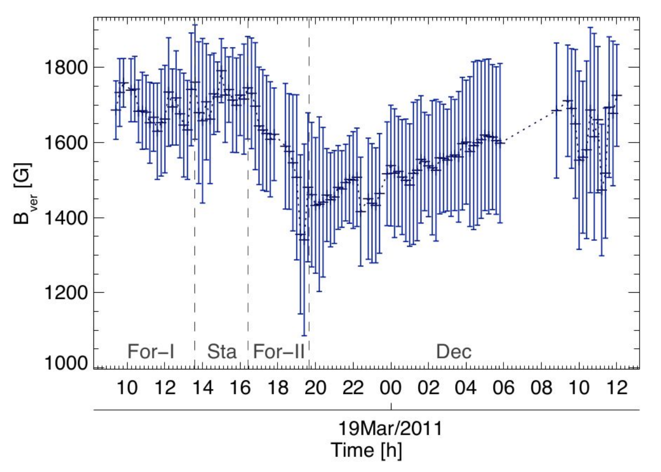

Figure 6: Temporal evolution of the averaged **parameters along the boundary** of the pore. Error lines represent the standard deviations. Vertical dashed lines separate the proposed evolutionary stages. *Top*: Magnetic field strength (***B***). *Bottom*: Vertical magnetic field (***B_{ver}***). [García-Rivas et al. 2021](#)

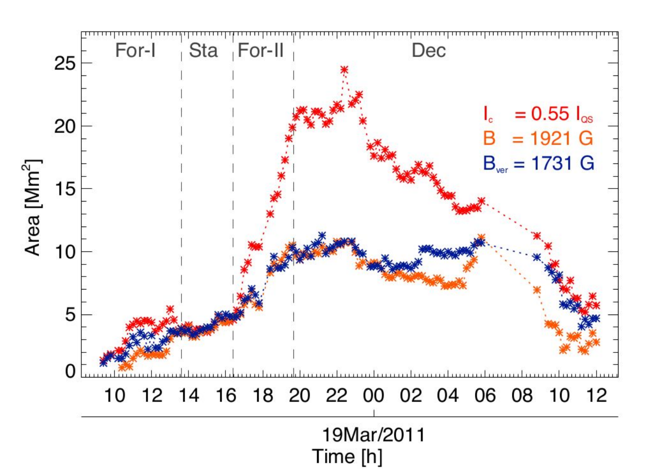

Figure 7: Temporal evolution of the **areas** encircled by **I_C= 0.55 I_{QS}** (red), **B_{crit} = 1921 G** (orange) and **$B_{ver,crit}$ = 1731 G** (blue). Vertical lines separate the proposed evolutionary stages.

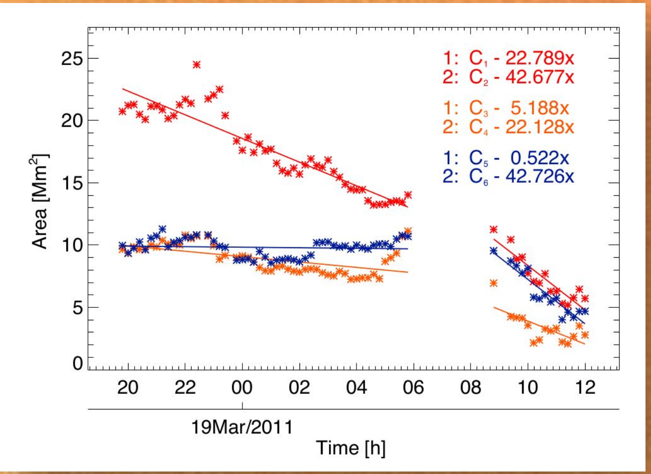

Figure 8: Decay rates of the **areas** encircled by **I_C= 0.55 I_{QS}** (red), **B_{crit} = 1921 G** (orange) and **$B_{ver,crit}$ = 1731 G** (blue). Lines represent the linear fit and the legend, the fitted coefficients.

Results

In this case study, the pore exhibits a **stable phase (Sta)**. The maximum B_{ver} value, observed during the stable phase, is comparable to the maximum B_{ver} value found on UP boundaries. Therefore, we consider the mean B and B_{ver} during the stability stage as **magnetic critical thresholds** for the analysis (**B_{crit} = 1921 G; $B_{ver,crit}$ = 1731 G**).

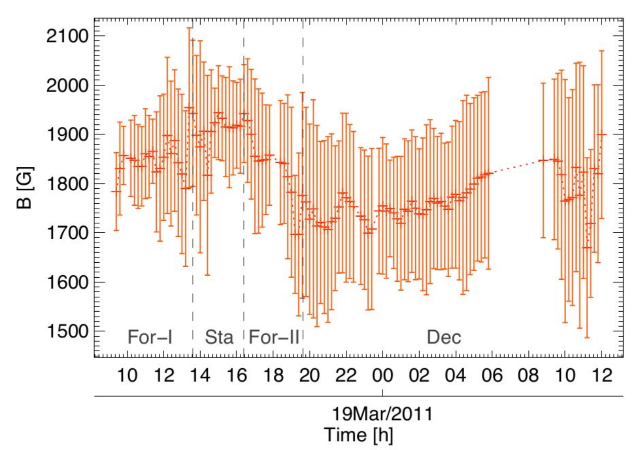

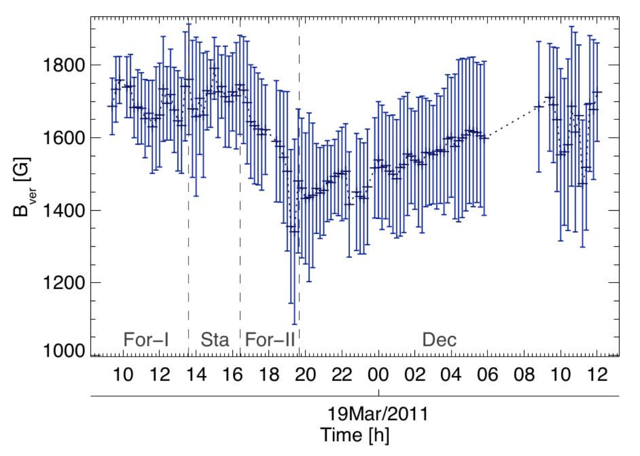

Figure 6: Temporal evolution of the averaged **parameters along the boundary** of the pore. Error lines represent the standard deviations. Vertical dashed lines separate the proposed evolutionary stages. *Top*: Magnetic field strength (***B***). *Bottom*: Vertical magnetic field (***B_{ver}***).

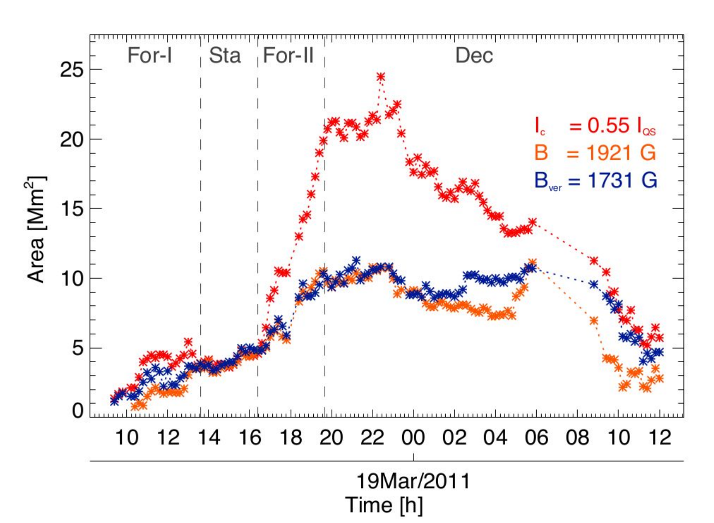

Figure 7: Temporal evolution of the **areas** encircled by **I_C= 0.55 I_{QS}** (red), **B_{crit} = 1921 G** (orange) and **$B_{ver,crit}$ = 1731 G** (blue). Vertical lines separate the proposed evolutionary stages. [García-Rivas et al. 2021]

The temporal evolution of the magnetic properties and areas of the pore present different **stages** in this case study:

- ***Formation I:*** The pore grows while |B| and B_{ver} increase.
- ***Stability***: The pore area evolves consistently with the areas limited by the magnetic thresholds.
- ***Formation II***: The pore grows steeply in the northern region of the pore with weaker and more horizontal field. |B| and B_{ver} strengthen in the pore but not enough, therefore, we see a decrease of |B| and B_{ver} on the boundary.
- ***Decay***: |B| and B_{ver} do not get strong enough in the newly emerged zone and it starts to decay. The northern region (with weaker |B| and B_{ver}) decays faster than the southern region.

Conclusions

- We find a **similar behaviour of B_{ver}** on **UP boundaries** and on **pores** during the evolutionary stages. We find a similar behaviour between **B_{ver}** and **|B|**.
- We find a **critical value** of the vertical magnetic field on pores.
- Only regions with **$|B_{ver}| < B_{ver,crit}$** are **occupied** by granulation (e.g. light bridge) in the lifetime of the pore.
- Regions with **$|B_{ver}| > B_{ver,crit}$** have, in general, **longer lifetimes** in the decay of a pore.
- In this case study, we find a similar behaviour between **B_{ver}** and **|B|**.

★ A **statistical analysis** is required to find out whether there is a critical value in other pores, whether |B| or B_{ver} is the stabilizing factor and its influence on pores lifetimes.

Related studies, e.g.: Benko et al. (2018), García-Rivas et al. (2021), Jurčák et al. (2020), Jurčák et al. (2017), Jurčák et al. (2015), Jurčák (2011), Lindner et al. (2020), Schamssmann et al. (2018)

<u>On-going analyses</u>: Transition sunspot - naked spots

The analysed sunspot appeared on the eastern limb in the active region **NOAA 12797** on 17 January 2021. Initially the sunspot was composed of two umbrae but, eventually, the penumbrae surrounding each umbrae separated permanently. The spots lost their penumbrae after 7 days -on 24 January- and the naked spots disappeared close to the western limb. We analysed these processes during **8 days**: from **00:00 UT on 19 January to 00:00 UT on 27 January 2021**.

Fig 8. Continuum intensity maps with intensity contour at 0.55Ic (white line). *First image*: sunspot on 19 January at 03:48 UT. *Second image*: decaying sunspots on 24 January at 04:36 UT. *Third image*: weak naked spots on 25 January at 02:00 UT. *Fourth image*: naked spots strengthened on 26 January at 01:36 UT.

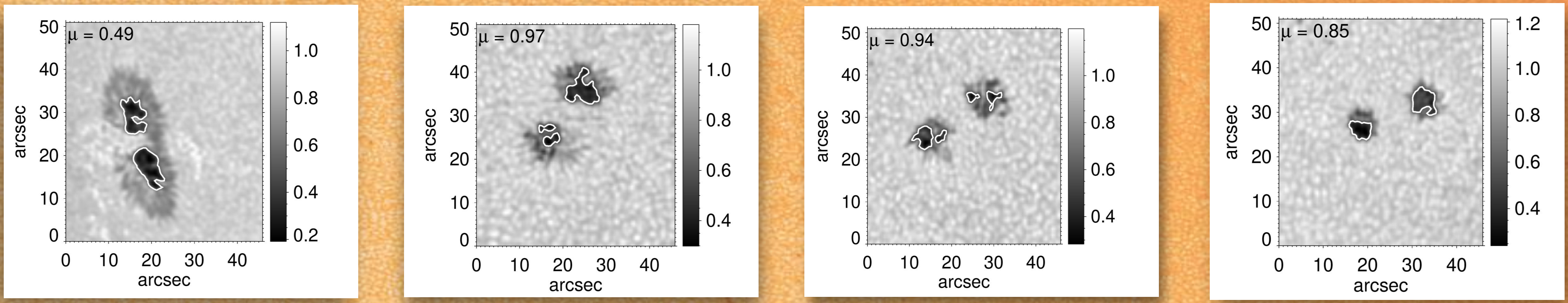

On-going analyses: Transition sunspot - naked spots

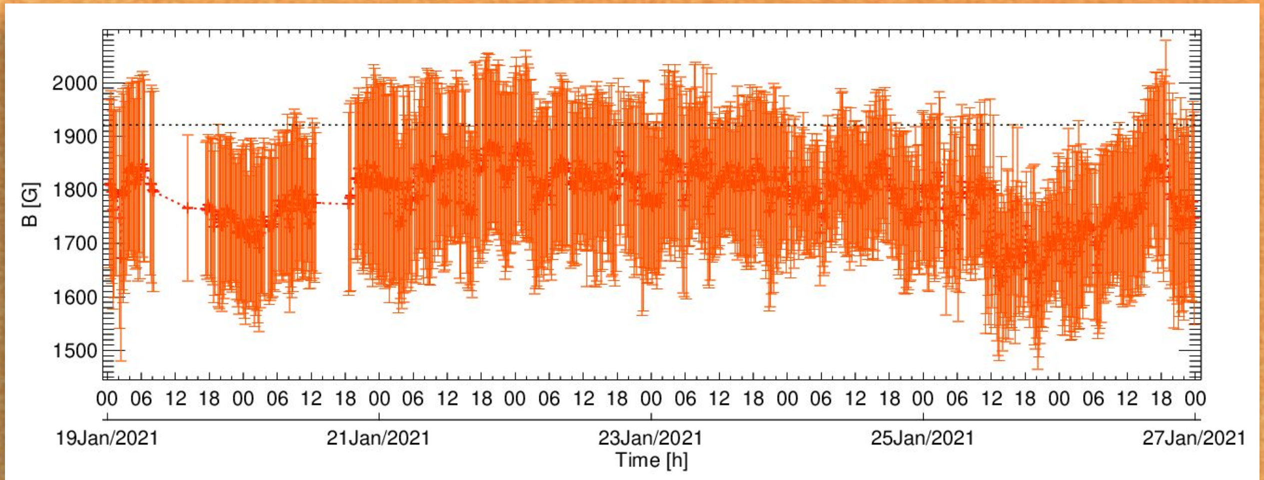

In this case study, the spots **do not exhibit a stable phase**. However, despite the decaying process, the **magnetic properties do not change significantly during the transition**. The naked spots undergo a weakening process (weaker magnetic field and irregular structure) after the disappearance of the penumbrae, followed by a strengthening process and permanent decay.

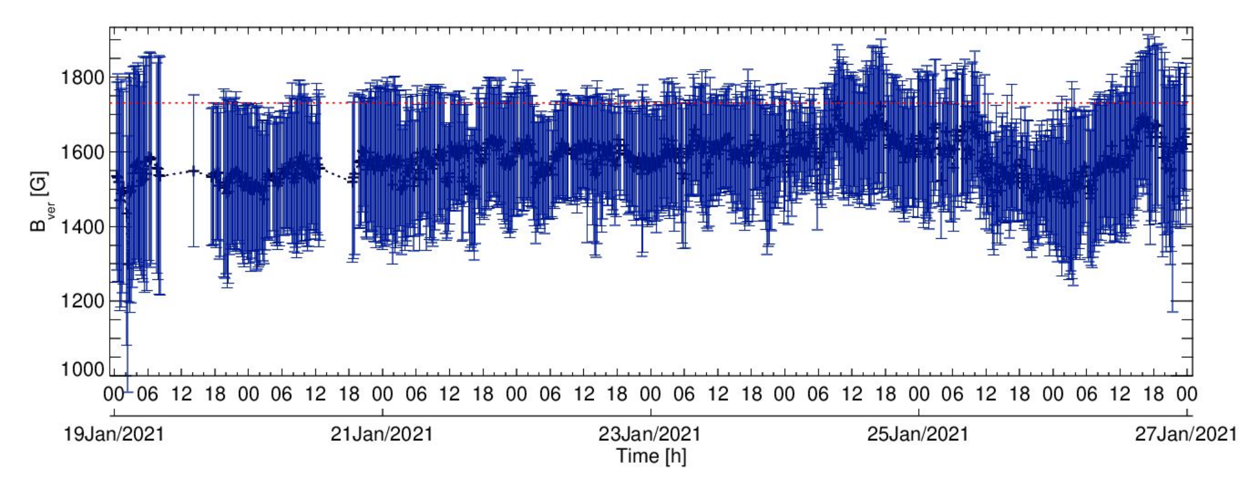

Figure 9: Temporal evolution of the averaged **parameters along the boundary** of the pore. Error lines represent the standard deviations. *Top*: Magnetic field strength (***B***). *Bottom*: Vertical magnetic field ($\boldsymbol{B_{ver}}$).